R-06-76

Validity document for COMP23

M Kelly, K A Cliffe
Serco Assurance

September 2006

Svensk Kärnbränslehantering AB
Swedish Nuclear Fuel
and Waste Management Co
Box 5864
SE-102 40 Stockholm Sweden
Tel 08-459 84 00
+46 8 459 84 00
Fax 08-661 57 19
+46 8 661 57 19

ISSN 1402-3091
SKB Rapport R-06-76

Validity document for COMP23

M Kelly, K A Cliffe
Serco Assurance

September 2006

Executive summary

The objective of this validity report is to demonstrate that the conceptual models, mathematical models and methods of solution adopted in COMP23 are fit-for-purpose for use in radioactive waste performance assessment calculations. This is achieved by:

1. Demonstrating that the conceptual models capture all of the important physical and chemical processes within the near field.
2. Showing that the governing equations and methods of solution are based on internationally accepted approaches.
3. Showing that areas of potential difficulty, for example flows from a narrow slit into a large compartment, are treated in an appropriate manner.
4. Demonstrating that COMP23 has undergone a thorough programme of verification and testing.

In addition, studies undertaken using the ENTWIFE code to investigate one of the analytical solutions employed in COMP23 are reported. These studies involved comparing the solutions to a diffusion problem obtained using COMP23 with those obtained with a fine-grid finite-element calculation. The level of agreement obtained in this study provides very strong evidence that the approach adopted in COMP23 is accurate and economical in terms of computing resources.

Neretnieks and his co-workers have recently produced a series of papers that consider in more detail the problem of groundwater and radionuclide flow into a narrow fracture, in particular the calculation of flow rates and equivalent flow rates. They proposed analytical solutions for these quantities that are shown to have excellent agreement with numerical simulations. This work is described herein.

Consideration should be given to the use of these updated analytical solutions in COMP23, maybe followed by the development of additional test cases to compare the results obtained with those from use of the current analytical solution.

Contents

1 Introduction

COMP23 is a fast, multiple-path model that calculates nuclide transport in the near field of a repository as occurring through a network of resistances and capacitances coupled together like an electrical circuit network. The model, which is a coarsely discretized, integrated finite-difference model, was designed to be fast and compact by making use of analytical solutions in sensitive zones. The code allows the user to simultaneously consider many pathways for nuclide transport, by advection and diffusion, to the flowing water in fractures surrounding the barrier system.

The nuclide dissolution may be calculated using either a solubility-limited approach or a congruent-dissolution approach. The conceptual model used in COMP23 can be represented by three bodies as shown in the figure below. The bodies are the source, the barrier system, and the sinks. The source is treated as a well-mixed compartment. The barrier system is the physical medium through which the nuclides migrate to reach the sinks located in the surrounding system, or outside of the region considered as the barrier system. The sinks, considered as recipients where the water flows, are fully defined by a local equivalent flow rate.

The purpose of this document is to provide confidence to future users of COMP23 that the model is fit-for-purpose and an appropriate tool for considering the containment, migration and transport of radionuclides through the near field of a repository. In Chapter 2, the conceptual basis and mathematical representation of the processes considered in COMP23 are set out. Throughout COMP23, well known and accepted assumptions, approximations and mathematical formulations are used. However, in some physical situations (for example diffusion from a small hole into a large compartment), standard approaches and approximations could lead to misleading or erroneous results. To circumvent this problem, COMP23 makes use of a number of analytical formulations to describe such situations. These analytical formulations are also set out in Chapter 3. Studies employed to verify the COMP23 approach are also described in Chapter 3.

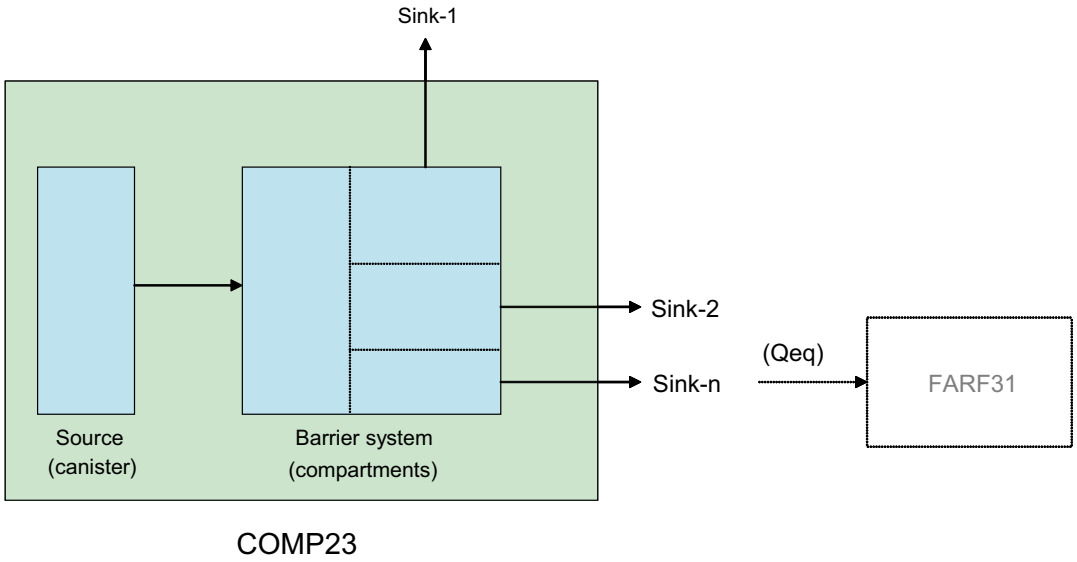

Figure 1-1. *The COMP23 and FARF31 models.*

In Chapter 4, the approach for solving the underlying equations is set out. The approach is based on the definition of a number of "compartments", with the main variables of interest being described in terms of average values within these compartments. This enables the governing equations to be solved using an integrated finite difference approach.

Chapters 5 and 6 provide direct evidence of the fitness-for-purpose of COMP23. In Chapter 5, the various verification and validation tests that have been applied to COMP23 framework are set out. These include tests that the various features of COMP23 work as intended, comparisons of the output results of COMP23 with the results from other codes, and tests against analytical solutions. In Chapter 6, the quality assurance status of the COMP23 code is described.

2 Mathematical model and boundary conditions

2.1 Radionuclide transport in the barrier

Radionuclides leaking from a damaged canister spread into the backfill material surrounding the canister and then migrate through different pathways into water-bearing fractures in the rock surrounding the repository. If the backfill and other materials surrounding the canister have a low permeability, the solute transport will be only by diffusion. If there is water flow through some zones of the barrier, then advection may also be a significant transport mechanism. Some solutes may be sorbed on the materials surrounding the canister along the transport paths and their migration will be retarded. Solutes may also precipitate. It is a basic assumption in the COMP23 model that the dissolution-precipitation reaction is very fast, so that, for nuclides that are solubility limited, the aqueous concentration will be at the solubility limit if there is any precipitate present. The COMP23 model allows groups of nuclides to share a solubility limit. For example, all the isotopes of a given element would be expected to share the same solubility limit.

The nuclides are labelled by consecutive integers, beginning with 1, in such a way that the parent of nuclide n, if it has one, is always nuclide $n-1$. Clearly nuclide 1 cannot have a parent. The fundamental equation expressing material balance for nuclide n is

$$\frac{\partial a^n}{\partial t} + \mathbf{u}_0 . \nabla c^n - \nabla \cdot D_e^n \nabla c^n = -\lambda_n a^n + \lambda_{n,.n-1} a^{n-1} \qquad (1)$$

where a^n is the total amount (dissolved, sorbed and precipitated) of nuclide n per unit volume, c^n is the concentration of nuclide n in the pore water, u_0 is the Darcy velocity, D_e^n is the effective diffusivity for nuclide n, λ_n is the decay constant for nuclide n and $\lambda_{n,n-1}$ is the decay constant for nuclide $n-1$ if nuclide n is the daughter of nuclide $n-1$ and zero if nuclide n does not have a parent. Note that the quantities a^n and c^n are functions of both position and time, and that u_0 and D_e^n may also depend on position.

Equation (1) is to be regarded as an equation for a^n, and so c^n must be specified as a function of a^n. To do this, the assumption that the precipitation/dissolution reaction is very fast is used. Each nuclide is considered to belong to a solubility group. Normally, there will be one solubility group for each different element and a group will consist of all the nuclides that are isotopes of a particular element. Let S_E denote the solubility group for element E. Then S_E is the set of labels of the nuclides that are isotopes of element E. The total amount of element E per unit volume is denoted by a_E^T and it is clear that

$$a_E^T = \sum_{m \in S_E} a^m . \qquad (2)$$

The concentration c^n, where $n\ n \in S_E$ (i.e. nuclide n is an isotope of element E), may now be related to a^n by:

$$c^n = \begin{cases} \dfrac{a^n}{K_E} & \text{if } a_E^T \le K_E c_E^S \\ \dfrac{c_E^S a^n}{a_E^T} & \text{if } a_E^T > K_E c_E^S \end{cases}, \qquad (3)$$

where K_E is a distribution coefficient for element E and c_E^S is the solubility limit for the solubility group, S_E, of element E. K_E is given by

$$K_E = \varphi_E + (1-\varphi_E)k_E^d \rho \quad (4)$$

where φ_E is the porosity for element E, ρ is the density of the solid material and k_E^d is the sorption coefficient for element E. The amount of nuclide n per unit volume that is in solution is $\varphi_E c^n$ and the amount that is sorbed is $(1-\varphi_E)k_E^d \rho$, so that the total amount, dissolved and sorbed, per unit volume is $K_E c^n$. Note that the COMP23 model allows the porosity to depend on the element, so that effects such as anion exclusion can be treated.

2.2 Treatment of the source term

In the COMP23 model, the radionuclides in the canister may be present in three forms: in solution in the water in the canister; in the form of precipitate in the canister and embedded in the fuel matrix. It is assumed that there is no sorption in the canister and that the time taken for the nuclides to mix in the canister is very short, so that the concentration of the dissolved nuclides is uniform. It is also assumed that the volume of water in the canister is constant during the calculation. As the fuel matrix dissolves, the actual volume available for the water in the canister will increase, but since the rate of dissolution is slow, this volume change can be neglected.

COMP23 treats three types of situation:

I Solubility limited approach. All species in the canister are available for release, independently of the structure they are part of. The only limitation in the nuclide release is the solubility of the individual species.

II A particular case for nuclides initially located at the fuel surface. The handling of this situation is similar to I but only a fraction of the total nuclide inventory is available for release.

III Congruent approach for nuclides embedded in a fuel matrix. Since the matrix is mostly formed by uranium oxide, the release rate for the embedded nuclides depends on the rate at which the uranium fuel matrix is dissolving. Several models are available to treat the dissolution of the fuel matrix and the effects of alpha-radiolytically induced dissolution can be treated. These different models are described in subsections 2.2.2 and 2.2.3.

2.2.1 Source term – solubility limited

The model for cases *I* and *II* is essentially the same. Case *I* is referred to as SOL_TYPE OWNSOL and case *II* as SOL_TYPE FUELSURFACE. Since the dissolved nuclides in the canister are assumed to be well mixed, the amount of each nuclide in the canister is determined by a single quantity, $\hat{a}^n$, that represents the total amount of nuclide in the canister and that is a function of time. The equation for nuclide n is:

$$\frac{\partial \hat{a}^n}{\partial t} = -\lambda_n \hat{a}^n + \lambda_{n,n-1}\hat{a}^{n-1} - f^n, \quad (5)$$

where f^n is the rate at which nuclide n leaves the canister by diffusion into the rest of the barrier system. If σ is the area of the canister that is breached, and so is in direct contact with the rest of the barrier system, then

$$f^n = -\int_\sigma D_e^n \mathbf{n}.\nabla c^n, \quad (6)$$

where $\mathbf{n}$ is the outward pointing normal to σ, and c^n is the concentration of nuclide n in the barrier system outside the canister, as in the previous section. Again, Equation (5) is to be regarded as an equation for $\hat{a}^n$. In order to determine f^n, and so complete Equation (5), the concentration of nuclide n in the canister, $\hat{c}^n$, must be provided as a boundary condition on σ for the nuclide transport equation outside the canister. The relationship between $\hat{a}^n$ and $\hat{c}^n$, where nuclide n is an isotope of element E, is

$$\hat{c}^n = \begin{cases} \dfrac{\hat{a}^n}{V_C} & \text{if } \hat{a}_E^T \le V_C c_E^S \\ \dfrac{c_E^S \hat{a}^n}{\hat{a}_E^T} & \text{if } \hat{a}_E^T > V_C c_E^S \end{cases}, \tag{7}$$

where V_C is the volume occupied by the water in the canister and $\hat{a}_E^T$ is the total amount of element E in the canister:

$$\hat{a}_E^T = \sum_{m \in S_E} \hat{a}^m. \tag{8}$$

The derivation of Equation (7) is similar to the derivation of Equation (3).

2.2.2 Source term – congruent release without alpha radiolysis

In Case *III*, which is referred to as SOL_TYPE MATRIX, the dissolution of the uranium fuel matrix, and the consequent liberation of the embedded nuclides, must be considered. In this case the quantity $\hat{a}^n$ represents the total amount of nuclide n that is in the canister, but is not embedded in the fuel matrix. In addition, it is necessary to keep track of the amount of nuclide embedded in the matrix, and this quantity is denoted by b^n. Note that both the $\hat{a}^n$ and b^n depend only on time. The equation for nuclide n becomes

$$\frac{\partial \hat{a}^n}{\partial t} = -\lambda_n \hat{a}^n + \lambda_{n,n-1} \hat{a}^{n-1} - f^n +, \tag{9}$$

where q^n is the rate at which nuclide n is being liberated from the fuel matrix, which is given, in terms of the rate at which the uranium matrix is dissolving, by

$$q^n = \frac{b^n}{b^M} q, \tag{10}$$

where b^M is the amount of uranium 238 in the fuel matrix, and q^M is the rate of dissolution of the uranium 238. The basic assumption underlying Equation (10) is that the nuclides are uniformly distributed within the fuel matrix, so that the ratio of the amount of nuclide n to the amount of matrix is uniform and equal to b^n/b^M. It is also assumed that all the nuclides embedded in the matrix are released when the matrix dissolves. Equation (10) follows immediately from these two assumptions.

The equation for the amount of nuclide n embedded in the matrix, b^n, is

$$\frac{\partial b^n}{\partial t} = -\lambda_n b^n + \lambda_{n,n-1} b^{n-1} - q^n. \tag{11}$$

Equations (9-11) can be used to determine $\hat{a}^n$ and b^n only once q^M is known. In COMP23, the way q^M is determined depends on whether alpha radiolysis is modelled or not. The case without alpha radiolysis is considered in this section. The case with alpha radiolysis is treated in subsection 2.2.3.

When alpha radiolysis is not included in the model, the rate of dissolution of the uranium matrix is determined by the solubility of the uranium in the canister. The model assumes that the rate at which the matrix dissolves is just fast enough to maintain the uranium in the water in the canister at its solubility limit without any precipitate forming. A faster rate of dissolution would obviously lead to the formation of uranium precipitate in the canister and a situation where the matrix would be dissolving rather than the precipitate, which is physically unreasonable (in the absence of effects such as alpha radiolysis) and contradicts the basic assumption that the rate of

dissolution of the precipitate is very fast. On the other hand, it is possible that the matrix could dissolve at a slower rate that is not sufficient to maintain the dissolved uranium at its solubility limit. However, the current assumption is conservative and leads to a well defined and relatively simple model.

Summing Equation (9) over all the isotopes of uranium and using Equation (10) gives

$$\frac{\partial}{\partial t}\sum_{m\in S_U}\hat{a}^m = \sum_{m\in S_U}\left(-\lambda_m a^m + \lambda_{m,m-1}\hat{a}^{m-1} - f^m\right) + \left(\sum_{m\in S_U} b^m\right)\frac{q^M}{b^M}. \tag{12}$$

Since the uranium in the water in the canister is at the solubility limit

$$\sum_{m\in S_U}\hat{a}^m = V_C\sum_{m\in S_U}\hat{c}^m = V_C c_U^S, \tag{13}$$

so that

$$\frac{\partial}{\partial t}\sum_{m\in S_U}\hat{a}^m = \frac{\partial}{\partial t}V_C c_U^S = 0. \tag{14}$$

Therefore

$$q^M = b^M\frac{\sum_{m\in S_U}\left(\lambda_m a^m - \lambda_{m,m-1}\hat{a}^{m-1} + f^m\right)}{\sum_{m\in S_U} b^m}. \tag{15}$$

To summarize, the model for congruent release of nuclides when there is no alpha radiolysis consists of Equation (9) for each nuclide except nuclide *M* (the uranium 238 matrix), Equation (11) for all nuclides and Equation (13), which effectively determines the amount of uranium in the canister that is not in the matrix. To complete these equations, q^n and q^M are given by Equations (10) and (15) respectively.

2.2.3 Source term – congruent release with alpha radiolysis

COMP23 can include the effects of alpha radiolysis on the spent fuel dissolution /Haworth et al. 1996, 1997/. The model assumes that the dissolution rate is related to the alpha-energy release of the fuel. When an alpha radiolysis model is used an instantaneous release fraction (IRF) can be specified for each embedded nuclide. This specifies the fraction of the nuclide that is assumed to dissolve instantaneously. Typically, as the matrix dissolves due to alpha radiolysis some of the uranium released will form as precipitate and the embedded nuclides will be freed to dissolve in the water.

Three different representations of the evolving alpha-energy release are included in COMP23.

- The dissolution rate of the fuel matrix occurs at a constant rate (CONSTANT type).
- The dissolution rate is a function of the alpha-radiolysis dose rate of the fuel, and decreases with time as a result of radioactive decay (DECAY type).
- The dissolution rate is a function of the alpha-radiolysis dose rate of the fuel, and decreases with time as a result of radioactive decay and dissolution of alpha-emitting solids from the fuel matrix (EXPLICIT type).

The alpha radiolysis model specifies the rate at which the uranium matrix dissolves due to alpha radiolysis, denoted by q_a^M. This rate can depend on time and on the amount of various alpha-emitting nuclides in the matrix, but is independent of the rate at which the uranium is leaving the canister, which is denoted by q_d^M.

$$q_d^M = b^M \frac{\sum_{m \in S_U} \left(\lambda_m \hat{a}^m - \lambda_{m,m-1} \hat{a}^m + f^m \right)}{\sum_{m \in S_U} b^m}. \tag{16}$$

The rate of dissolution of the uranium matrix, q^M, is specified by

$$q^M = \begin{cases} q_d^M & \text{if } \hat{a}_U^T \le V_C c_U^S \\ q_\alpha^M & \text{if } \hat{a}_U^T > V_C c_U^S \end{cases} \tag{17}$$

When the effects of alpha radiolysis are included in the model, the rate of dissolution of the uranium matrix is always at least the alpha-radiolysis rate. If there is uranium precipitate in the canister and $q_a^M < q_d^M$, the amount of precipitate will decrease until such time as either $q_a^M \ge q_d^M$, or else all the uranium precipitate has been dissolved. The rate of dissolution of uranium will still be q_a^M during this period because the precipitate dissolves much more readily than the matrix. Once all the uranium precipitate in the canister has been dissolved, it is assumed that the rate of matrix dissolution will be such as to keep the concentration of uranium in the water at the solubility limit, provided that $q_a^M < q_d^M$ still holds. This implies that the rate of dissolution is equal to the rate at which uranium is leaving the canister, q_d^M. As was pointed out in subsection 2.2.2, this particular assumption is conservative. Note that the uranium concentration in the canister cannot drop below its solubility limit until the entire uranium matrix has been dissolved (which would take a very long time in most situations).

The three models for the alpha-radiolysis dissolution rate, q_a^M, are:

Constant

$$q_a^M = K_{CON}\,, \tag{18}$$

where K_{CON} is a constant.

Decay

$$q_\alpha^M = K_{DEC} \sum_{i=1}^{4} A_i \exp\left(-\frac{t \ln 2}{B_i} \right), \tag{19}$$

where K_{DEC} is a constant, t is the time, and A_i, B_i, $i = 1,...,4$ are constants specific to the nuclides Am-241, Pu-239, Pu-240 and Np-237 in a particular fuel type /Werme et al. 1990/. If a different fuel to that described in reference /Werme et al. 1990/ is used, the constants will need to be changed in the program. However, it is not likely that this model will be used extensively as the CONSTANT model provides an adequate representation of dissolution. The constants, obtained from reference /Werme et al. 1990/, are given in the table below (Table 2-1).

Explicit

$$q_{\alpha}^{M} = K_{EXP} \sum_{m \in \Gamma} C_m b^m \qquad (20)$$

where K_{EXP} is a constant, Γ is the set of nuclide labels for the alpha-emitting nuclides, C_m are constants corresponding to the nuclides in Γ, and b^m is the amount of nuclide m in the fuel matrix. This model is included to allow flexibility of the program. In the current version of the program the nuclides Am-241, Pu-239, Pu-240 and Np-237 are included and the values of the constants, obtained from reference /Werme et al. 1990/, are given in the table below (Table 2-2).

To summarize, the form of the equations representing the model for congruent release of nuclides including alpha radiolysis depends on whether there is uranium precipitate in the canister or not. When uranium precipitate is present in the canister the model consists of Equations (9) and (11) for all nuclides together with Equations (10) and the second part of (17). When there is no uranium precipitate present, the model is the same as the case when there is no alpha radiolysis, described in subsection 2.2.2.

Table 2-1.

Nuclide	A_i	B_i
Am-241	25.3	433
Np-237	0.04	$2.1 \cdot 10^{6}$
Pu-239	1.1	$2.4 \cdot 10^{4}$
Pu-240	2.2	6,570

Table 2-2.

Nuclide	C
Am-241	2.85
Np-237	$8.81 \cdot 10^{-3}$
Pu-239	0.0261
Pu-240	0.0992

3 Analytic solutions used in the model

A number of analytic solutions are used in COMP23, in order to handle situations where numerical difficulties might arise. These include

- transport by diffusion into the flowing water,
- transport of solute through a small contacting area into a large volume compartment,
- transport of solute into a narrow slit /Romero et al. 1995/.

Other approaches could be included in the code in the future. In this section, the analytic solutions are discussed, the outcome of a verification exercise using Serco Assurance's ENTWIFE code are presented, and recent work on analytic solutions for a fracture intersecting a canister deposition hole are discussed.

3.1 Analytic solutions incorporated into COMP23

3.1.1 Transport into flowing water

For compartments in contact with water flowing in fractures in the rock, the diffusive transport is determined by an equivalent flow rate Q_{eq}. This parameter is a fictitious flow rate of water that carries with it a concentration equal to that at the compartment interface, and is therefore given by

$$N = Q_{eq}\,(c_1 - c_\infty) \tag{21}$$

where N is the actual flux of radionuclides by diffusion out of the compartment in contact with flowing water, c_1 is the concentration at the compartment interface and c_∞ is the concentration of radionuclides in flowing water past the compartment.

For a cylindrical canister surrounded by bentonite backfill, Neretnieks /Neretnieks 1982/ has shown that the mass flux by diffusion into flowing water is given by

$$N = 2\pi rL\varphi(c_1 - c_\infty)\sqrt{\frac{4D}{\pi T}} \tag{22}$$

where r is the radius of the canister/bentonite system, L is the canister height, D is the diffusivity of flowing water, T is the residence time for water contact with the bentonite and φ is the porosity of the bedrock in which water flows. This formula is obtained by solving the diffusion equation with appropriate boundary and initial conditions. This expression also assumes that the penetration depth of radionuclides into flowing water is small compared with the length of flow along the bentonite compartment.

The time of residence T is obtained by evaluating the time required for water to travel half a circumference of the canister/bentonite cylinder. Thus

$$T = \frac{\pi r\varphi}{q} \tag{23}$$

where q is the Darcy velocity of the flowing water. Eliminating the porosity φ from (22) gives

$$N = 2qL(c_1 - c_\infty)\sqrt{\frac{4DT}{\pi}} \tag{24}$$

and hence the equivalent flow rate is given by

$$Q_{eq} = 2qL\sqrt{\frac{4DT}{\pi}} \tag{25}$$

This expression may be re-written by eliminating the residence time. The result is an expression that gives the equivalent flow rate as proportional to the square root of the Darcy velocity. In COMP23, the equivalent flow rate is specified as follows:

$$Q_{eq} = constant \times q^n \tag{26}$$

where *n* and *constant* are to be supplied by the user. However, from Equation (25) it can be seen that these quantities are easily obtained. Of course, these values need not be used if an alternative approach is available. In some calculations, it is convenient to obtain the effective flow rate directly from Connectflow or a similar code and read these into COMP23 from a PTABLE.

In Section 3.3, some recent work undertaken by Neretnieks and his co-workers is presented. This work extends the derivation of Q_{eq} values and shows that there are other analytic solutions that are valid for a variety of fracture types that intersect a canister.

3.1.2 Transport into a large compartment

Species diffusing out of a small hole into a very large volume of material spread out spherically. Very near the hole, the cross-section is still of the order of the size of the hole. Further away, the cross section increases considerably as the "sphere" grows. Thus, most of the resistance to diffusion is concentrated very near the mouth of the hole. This resistance is calculated by integrating the transport rate equation:

$$N = -2\pi r^2 D_e \frac{dc}{dr}, \tag{27}$$

from a small hemisphere into a very large volume, between the limits of the sphere of radius r_{sph} and an outer radius *r*. Since the species spread over a large volume in the surrounding medium ($r >> r_{sph}$), the nuclide transport rate simplifies to

$$N = 2\pi r_{sph} D_e \Delta c \tag{28}$$

In the model, the real situation is approximated by using an equivalent plug. This plug of a cross-sectional area equal to the hole area has a thickness Δx given by

$$\Delta x = r_{hole} / \sqrt{2}. \tag{29}$$

In Section 3.2, the results of some additional calculations undertaken with the ENTWIFE code are presented that verify the adequacy of this approach.

3.1.3 Transport into a narrow slit

For the diffusive transport into a narrow fracture, most of the resistance to the transport will be located nearest to the fracture because of the contraction in the cross-sectional area. The transport resistance is then approximated by a plug through which the nuclides are transported. The plug has a transport area equal to the cross-sectional area of the fracture, and a diffusion length equal to a factor times the fracture aperture. Neretnieks analytically modelled the stationary transport from the bentonite surrounding a canister for spent nuclear fuel into a fracture /Neretnieks 1986/. His analysis considers the transport system shown in the following figures. Note that these are reproduced directly from /Neretnieks 1986/.

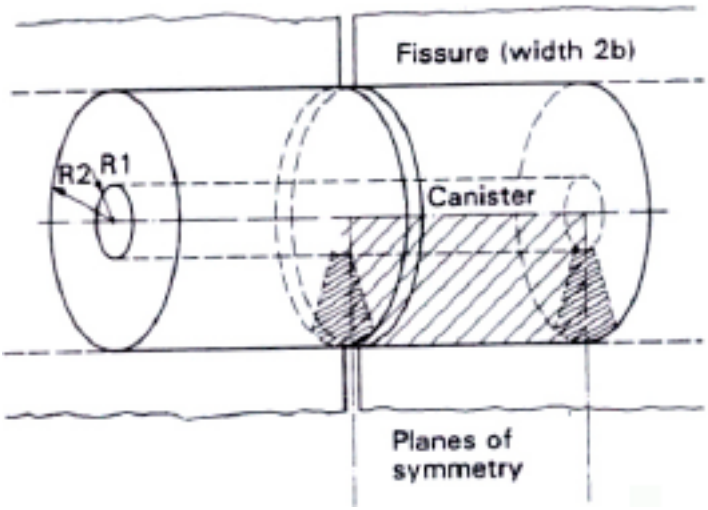

Figure 3-1. *This figure shows a fracture intersecting a deposition tunnel, along with the canister and bentonite in a deposition borehole.*

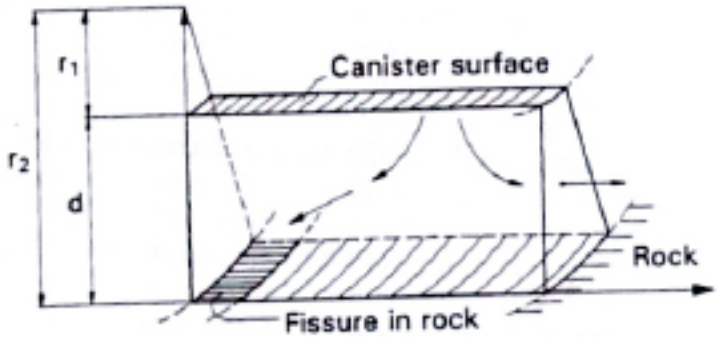

Figure 3-2. *This figure shows the flow of radionuclides in such a system, from canister to fracture.*

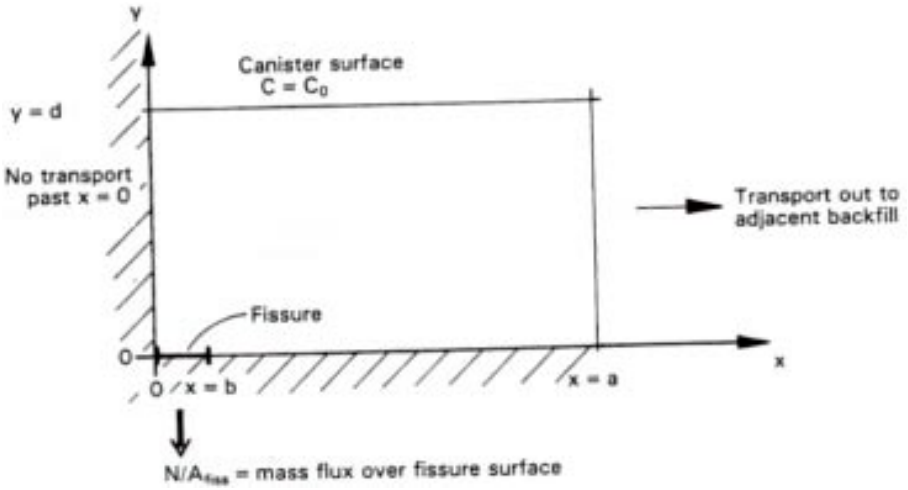

Figure 3-3. *This figure shows the stylised system to be considered for analysis. The cylindrical section of the previous figure is replaced by a rectangle, so that the diffusion equation can be written in Cartesian co-ordinates. The fracture into which radionuclides flow is represented by the region* $0 <= x <= b$, $y = 0$.

Neretnieks determined the following equation and boundary conditions to represent the concentration c of radionuclides due to steady state diffusion from the canister, through the bentonite and into the fracture:

$$\frac{\partial^2 c}{\partial x^2} + \frac{\partial^2 c}{\partial y^2} = 0 \qquad (30)$$

with

$$\frac{\partial c}{\partial x} = 0 \qquad \text{at } x = 0 \qquad (31)$$

and

$$\frac{\partial c}{\partial x} = -kx \qquad \text{at } x = \text{a} \qquad (32)$$

and

$$\frac{\partial c}{\partial y} = f(x) \qquad \text{at } y = 0 \qquad (33)$$

and

$$c = c_0 \qquad \text{at } y = d \text{ (the canister wall)} \qquad (34)$$

Neretnieks showed that the solution of this system of equations could be written in the form

$$c = c_o - \frac{N}{A_{frac} D_{Bent}} F(x,y) \qquad (35)$$

where $F(x,y)$ is a complicated function of the spatial co-ordinates x and y and other system dimensions and properties.

If the concentration at the fracture opening, i.e. for $0 <= x <= b$, $y = 0$, is constant across the fracture opening and equal to c_1, then this implies that the rate of flow through the fracture opening is

$$N = \frac{D_{Bent}\, A_{frac} (c_0 - c_1)}{F(x,0)} \qquad (36)$$

Thus, $F(x,0)$ can be considered as an effective thickness of material that, over the width of the fracture opening, provides the same resistance to diffusion as the whole region $0 < x < a$ and $o < x < b$. The diffusional resistance associated with this flow can be written in the form

$$R_{Diff} = \frac{F(x,0)}{D_{Bent}\, A_{frac}} = \frac{(F(x,0)/b)b}{D_{Bent}\, A_{frac}} \qquad (37)$$

The reason for the second form of the diffusional resistance in the above equation is that Neretnieks undertook some further studies, to examine how the function $F(x,0)/b$ varies as the various system dimensions are varied. The results are shown in the following figure, again taken directly from /Neretnieks 1986/.

This plot (Figure 3-4) shows that the value of $F(x,0)$ is fairly insensitive to the ratio of the fracture aperture to the canister length, over a number of orders of magnitude variation in this ratio. The same also applies for variations in the ratio of the backfill thickness to the canister length. Neretnieks has shown that in the regime $10^{-6} < b/a < 10^{-1}$ and $0.03 < d/a < 1$, the function $F(x,0)$ is well approximated by

$$F(x,0)/b = 1 - 1.35\log(b/a) + 1.6\log(d/a) \qquad (38)$$

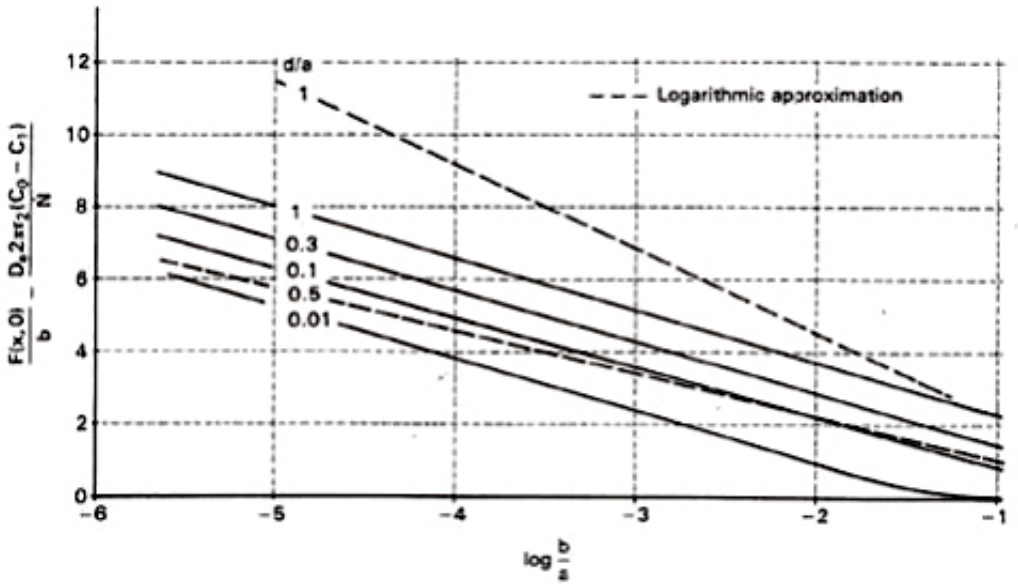

Figure 3-4. *Narrow slit approximation.*

In the context of COMP23, the analysis undertaken by Neretnieks is of great importance, as it demonstrates that flow into a narrow fracture can be represented by a plug that provides a diffusional resistance given by Equation (37). In addition, the required length of the plug can be represented by simple formulae that are valid over a very wide range of backfill thicknesses and fracture apertures. The cross-sectional area of the plug is equal to the fracture aperture cross-section.

3.2 Comparisons with ENTWIFE

In subsection 3.1.2, the approach for dealing with transport out of a small hole into a very large compartment is described. In the COMP23 model, this situation arises when radionuclides diffuse out of a small hole in a canister into the surrounding bentonite. In such situations, the ratio of the area of the region into which radionuclides diffuse to the area of the hole could be a factor of 10^6 or more. In order to provide accurate results using a numerical solution scheme (e.g. using finite elements), a very fine grid would be required in the region of the hole. This would require considerable computational resources, and as such is not considered a feasible means of dealing with diffusion from a small hole into a large container.

As described in subsection 3.1.2, the solution to this problem in COMP23 is to associated an additional diffusional resistance with the hole. The rationale for doing this is that most of the resistance to diffusion will be associated with the hole, on account of the small cross-sectional area compared with the compartment into which radionuclides diffuse. The extra resistance is computed from a steady state analytic solution of the diffusion equation, under the conditions of spherical symmetry (i.e. neglecting the boundaries of the bentonite compartment) and is given by

$$R_{hole} = \frac{1}{D_{bentonite}\sqrt{2\pi A_{hole}}} \tag{39}$$

However, in practice the diffusion into bentonite will need to be considered over all timescales and for a bentonite compartment with a finite geometry and dimensions. The question, therefore, is how good is this relatively simple approach for non-steady state diffusion and diffusion into a compartment with finite boundaries.

In order to answer this question, Serco Assurance used the ENTWIFE /Serco Assurance/ computer code to undertake some detailed finite element calculations of diffusion from a small hole into a large compartment. These calculations were then compared with some corresponding runs of COMP23, to see how well the results agreed with the ENTWIFE simulations.

Briefly, ENTWIFE is a finite-element computer program for solving systems of second-order elliptic differential equations. It has extensive capabilities for analysing nonlinear problems that may exhibit bifurcation phenomena. The program can be used to compute solution branches, various bifurcation points, and paths of bifurcation points. It can also be used to examine the stability of previously computed solutions using eigenvalue techniques. A preprocessor, called ENTCODE, is available for ENTWIFE. ENTCODE provides an interface to computer algebra packages (Mathematica and REDUCE are supported at the moment) that can be used to generate the FORTRAN subroutines that ENTWIFE needs to specify the governing equations of the problem under study. ENTCODE gives ENTWIFE a great deal of flexibility. ENTWIFE will run on most Unix workstations, including Intel based machines running Linux. ENTWIFE belongs to the same stable of codes as NAMMU and NAPSAC, and has been tested and applied extensively over a number of years /Serco Assurance/.

Two sets of calculations were undertaken with ENTWIFE. These are:

1. Diffusion from a small cylinder into a larger cylinder.
2. Diffusion from a small cylinder into a square box.

The first case has axial symmetry, whereas the second case is a full three-dimensional diffusion problem. These two cases are illustrated in Figure 3-5.

A number of sub-cases were considered in which the ratio of the area of the area of the larger compartment to the area of the cylinder (which represents the hole through which diffusion occurs) is varied. Area ratios were varied from 10^3 to 10^6. This was implemented by considering a small cylinder with a hole of unit radius, and a box or larger cylinder with dimensions ranging from 312.5 down to 9.8 (equal to 312.5/32).

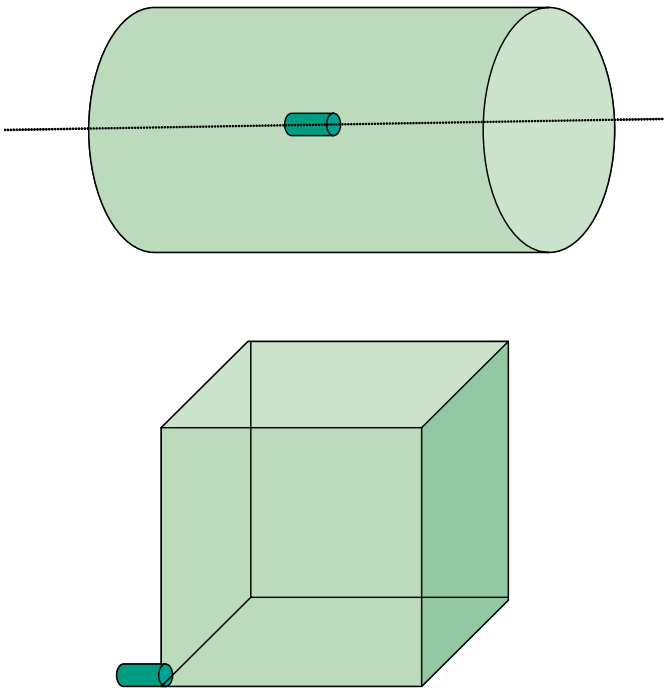

Figure 3-5. *ENTWIFE calculation cases.*

One of the main issues in producing the ENTWIFE simulations is to build a suitable grid on which to base the calculations. In the following discussion, attention is focused on the three-dimensional case of flow from a cylinder into a square box. The following figure (Figure 3-6) shows a cross-section of the grid used to simulate the diffusion from a cylinder into a square box.

It can be seen that near the cylinder through which radionuclides diffuse (bottom left), the grid is necessarily quite fine, in order to ensure acceptable accuracy in the simulations. Further away from the cylinder, the grid spacing is greater, as such a fine grid is not required in these regions. On the basis of this grid, the diffusion equation is solved in ENTWIFE using Gear's method for transients.

The figures on the following pages illustrate the solution for contaminant concentration as a function of time, displayed as contours of constant concentration.

In order to make a comparison with the results produced by COMP23, a number of COMP23 simulations were undertaken to match the cases computed with ENTWIFE. Each COMP23 model consisted of nine compartments. The first compartment was used as a container for a large amount if U-238 at a solubility limit of 1 mol m^{-3}. The second compartment was used to mimic the small cylinder, and the remaining compartments were used to mimic either the larger cylinder or the square box, depending on the case being considered.

The first compartment provides effectively a continuous source of radionuclide at unit concentration, which in turn diffuses into the smaller cylinder. Radionuclides then diffuse from the smaller cylinder into the other compartments. Because of the geometry of the two systems being modelled, care needs to be taken to ensure that appropriate diffusion lengths and cross-sectional areas are chosen in the COMP23 model.

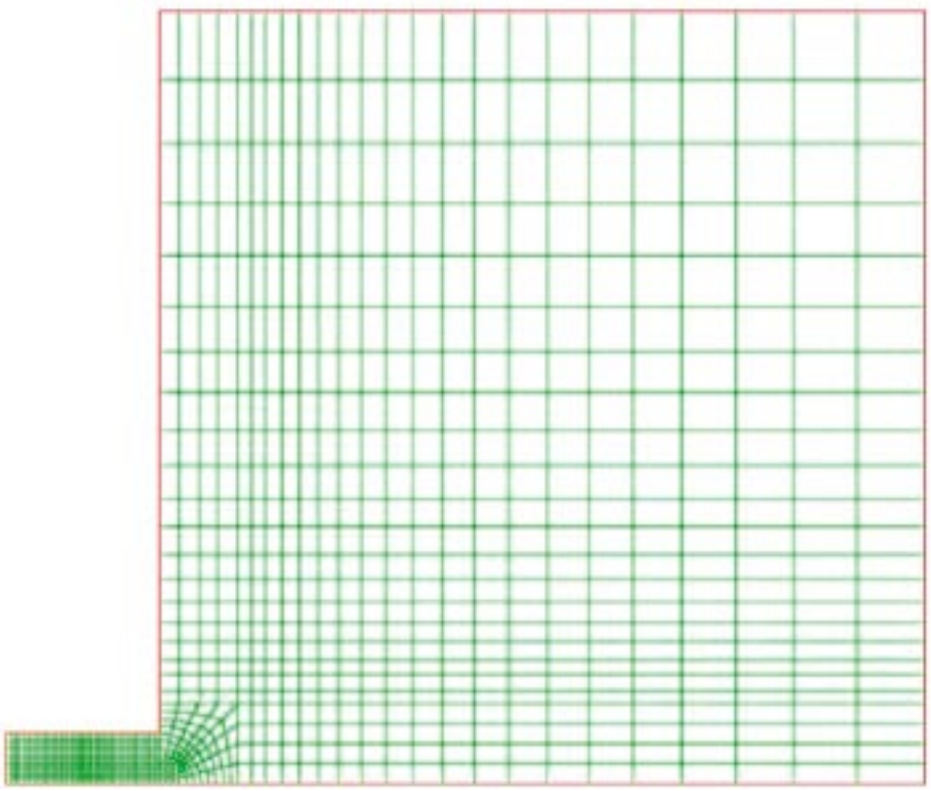

Figure 3-6. *ENTWIFE grid.*

Figure 3-7. *This figure shows the initial state of the system, before any diffusion into the box occurs.*

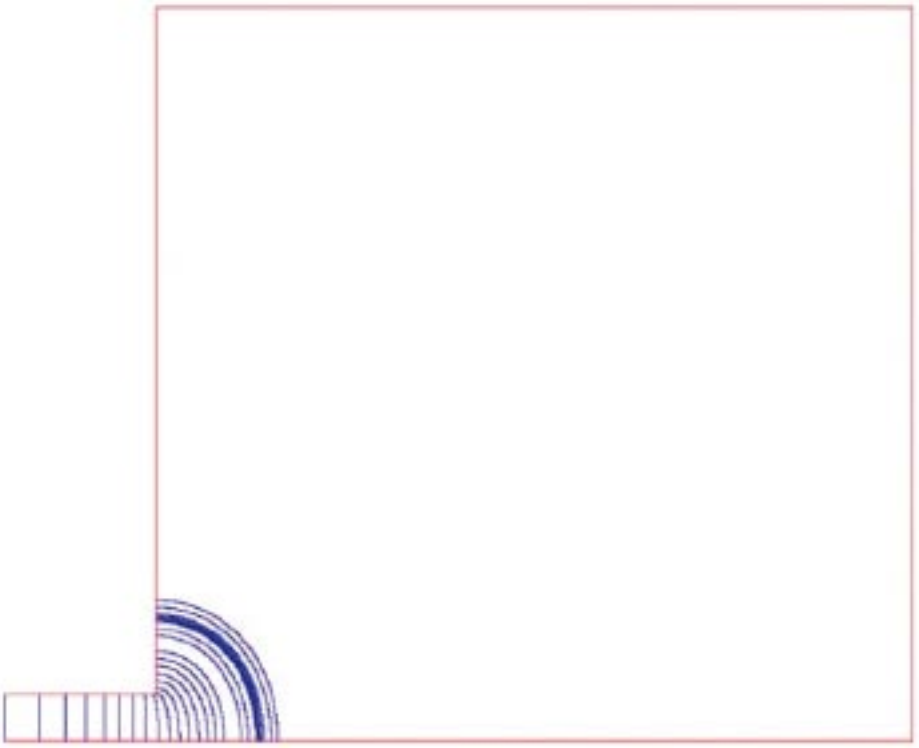

Figure 3-8. *Initially, the concentration contours are spherical within the large box. This is to be expected, as the diffusion distance is small compared to the dimensions of the box.*

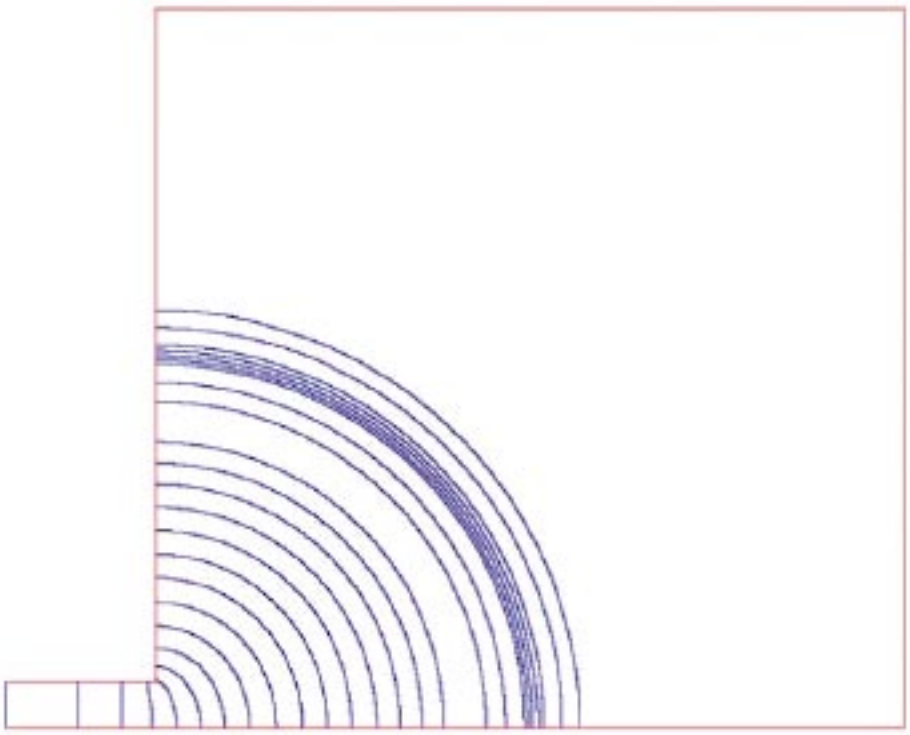

Figure 3-9. *The concentration contours remain spherical at longer times, as the diffusion distance is still smaller than the dimensions of the box.*

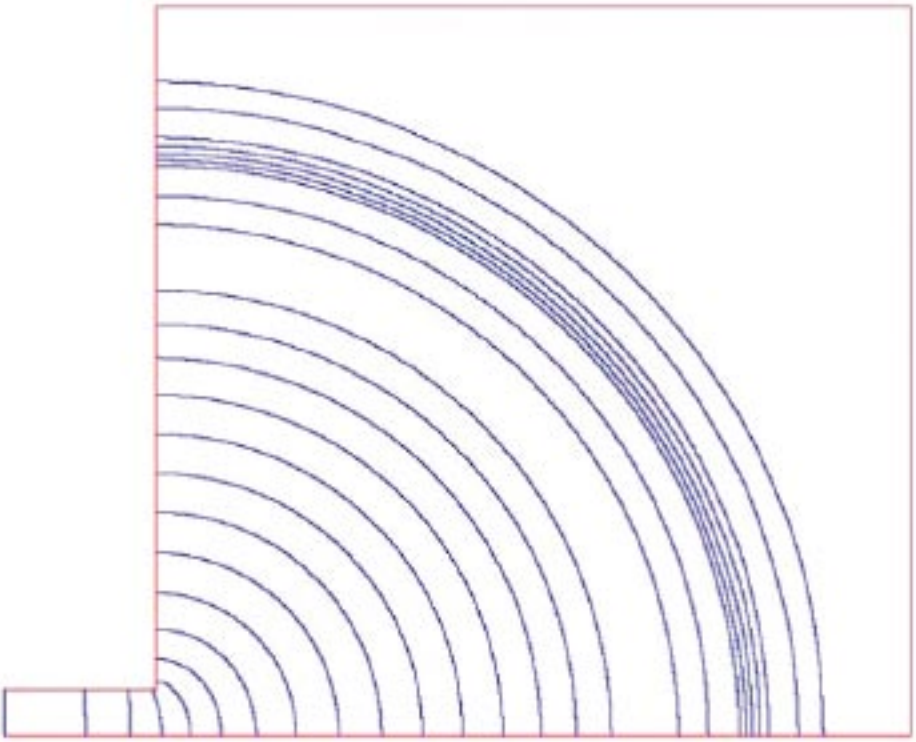

Figure 3-10. *The concentration contours remain spherical at substantial diffusion distances into the box.*

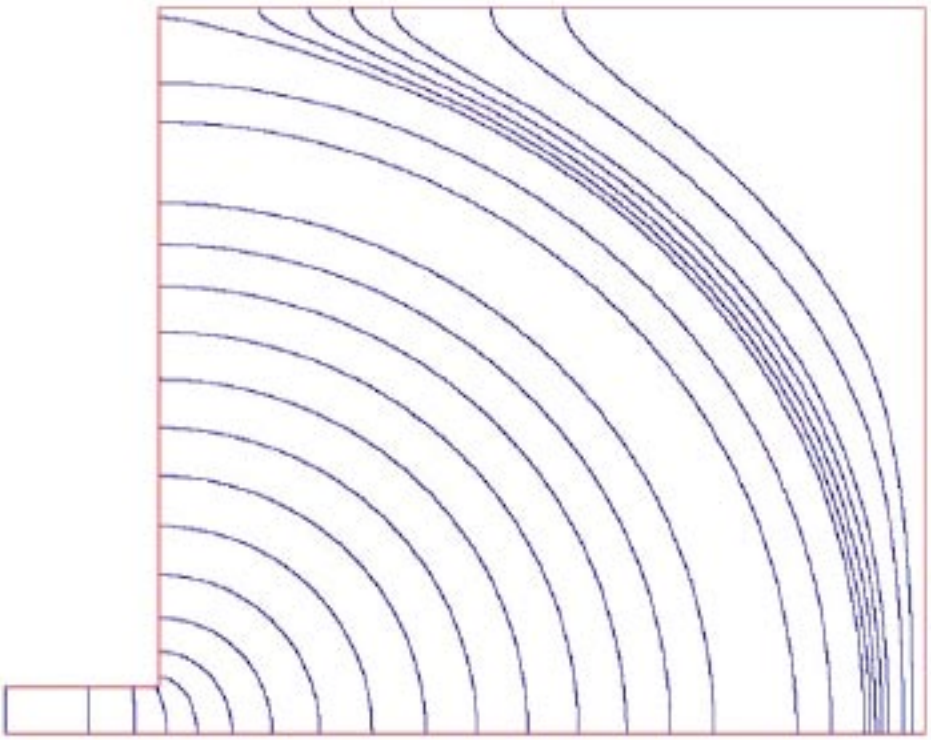

Figure 3-11. *As the distance of diffusion approaches that of the dimensions of the box, edge effects start to become apparent.*

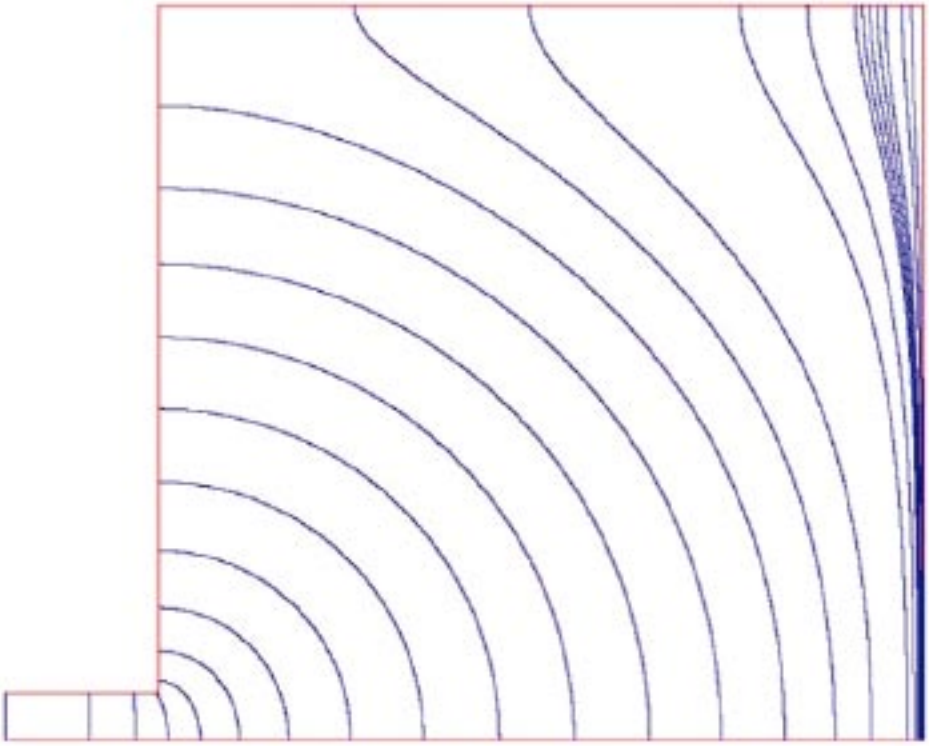

Figure 3-12. *At still greater times, the concentration contours near the edge of the box depart completely from being spherical.*

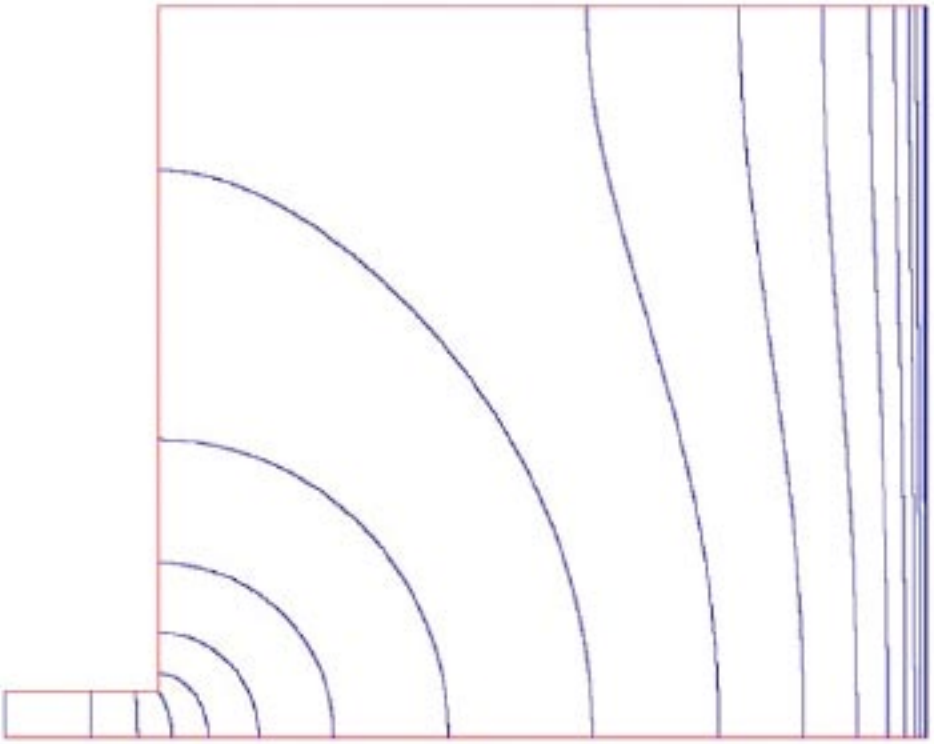

Figure 3-13. *In this figure it can be seen that close to the hole (cylinder), the concentration contours are spherical. However, far away from the hole where edge effects are important, the contours are governed by the properties of the edge of the box.*

The following figures indicate the comparison between the results obtained using ENTWIFE and the results obtained from the COMP23 simulations. In order to make this comparison, the ENTWIFE results were integrated over the volumes of the compartments used in COMP23, in order to produce concentrations that could be compared with the results from the COMP23 simulations.

In all of the following figures (Figure 3-14 to Figure 3-19), the continuous lines are the ENTWIFE results and the crosses represent the output from COMP23. Results are presented for the seven COMP23 compartments used to represent the large cylinder or box.

On the basis of these results, it can be concluded that the approach adopted in COMP23, i.e. the use of an additional diffusional resistance to model the effects of flow from a small hole into a large compartment, is an extremely effective and accurate means of tackling the problem. With this approach, it is not necessary to use very fine grids to model the diffusion in the vicinity of the small hole, and provides further evidence that COMP23 is fit-for-purpose for modelling such problems.

The general level of agreement between COMP23 and ENTWIFE seems to be best when the hole size is small relative to the size of the larger compartment. However, it is in such circumstances that most of the diffusional resistance is associated with the small hole, and hence the approach adopted in COMP23 has the greatest validity. Nevertheless, the level of agreement is perfectly acceptable for all practical applications of COMP23 to radionuclide migration and transport problems.

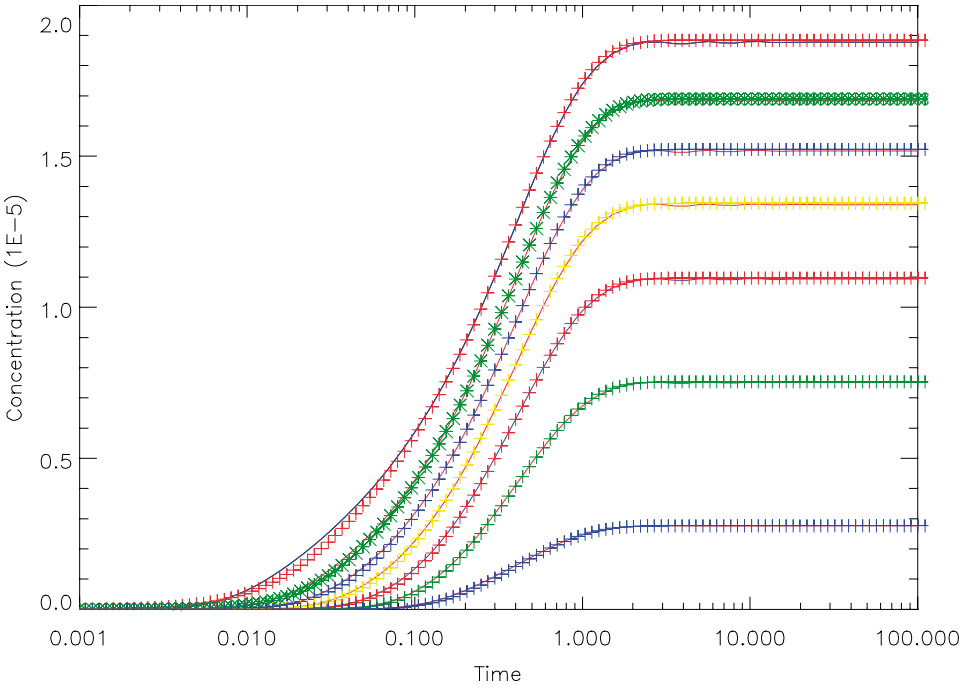

Figure 3-14. *This first figure illustrates diffusion into a larger cylinder, with unit hole radius and relative cylinder dimension of 312.5. Agreement is excellent.*

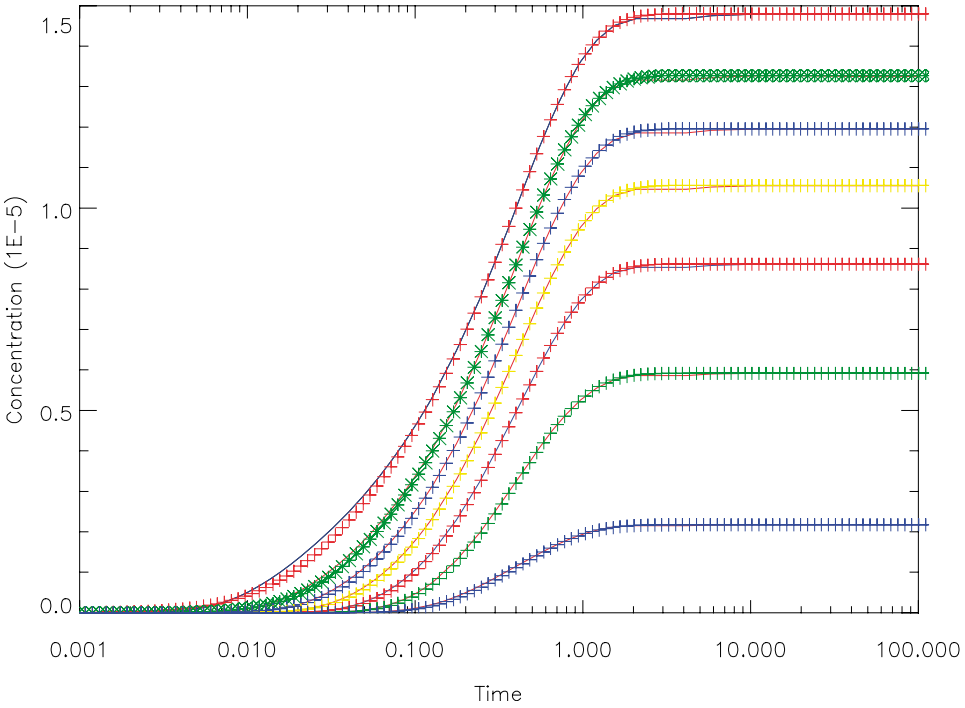

Figure 3-15. *This figure illustrates diffusion into a larger box, with unit hole radius and relative box dimension of 312.5. Agreement is excellent.*

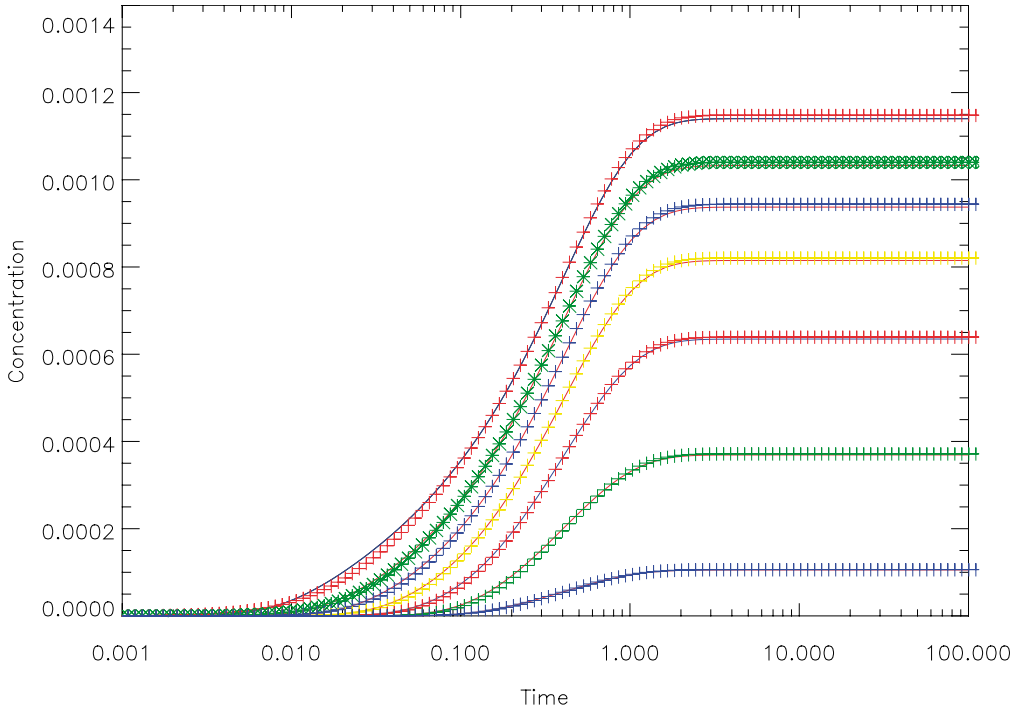

Figure 3-16. *This figure illustrates diffusion into a larger cylinder, with unit hole radius and relative cylinder dimension of 312.5/8. Agreement is again excellent.*

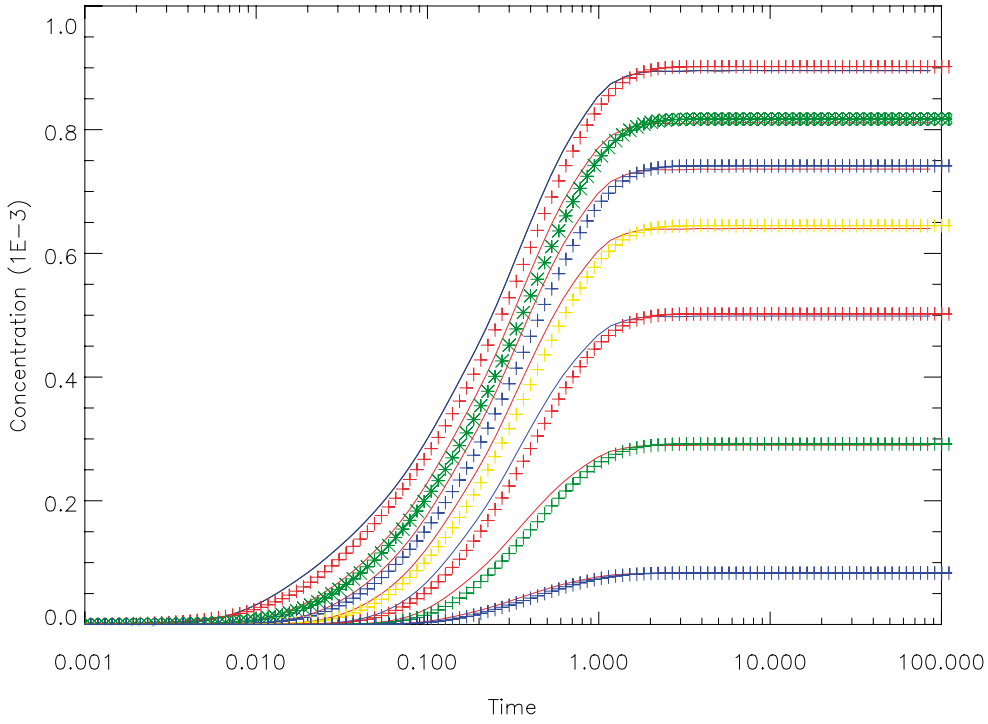

Figure 3-17. *This figure illustrates diffusion into a larger box, with unit hole radius and relative cylinder dimension of 312.5/8. Agreement is good, but not as good as for the previous cases considered.*

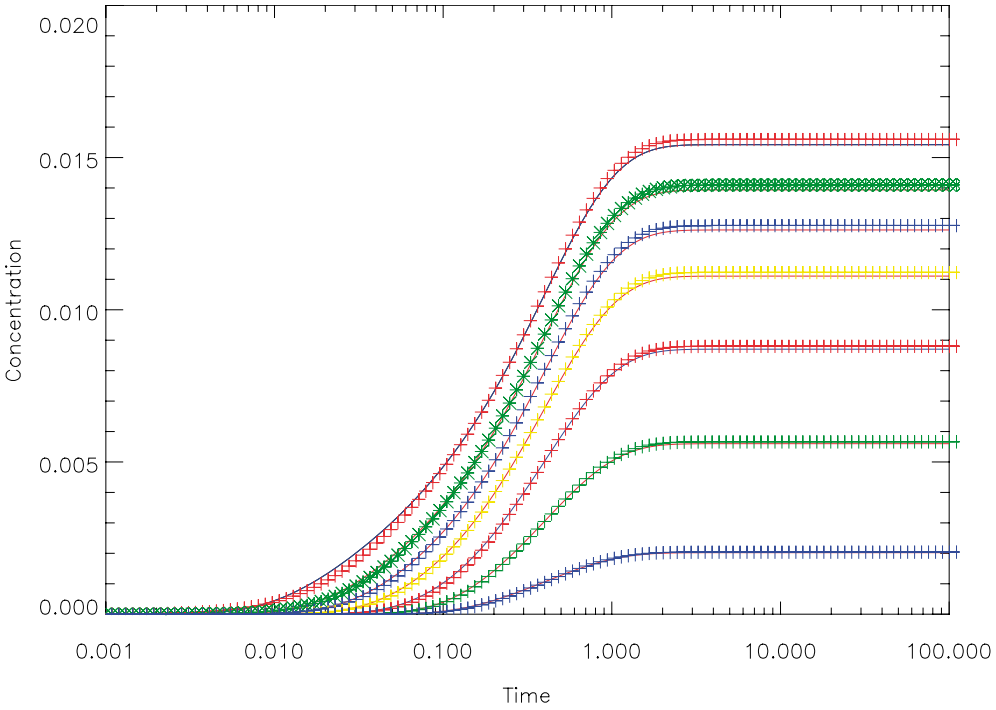

Figure 3-18. *This figure illustrates diffusion into a larger cylinder, with unit hole radius and relative cylinder dimension of 312.5/32. Agreement is again excellent.*

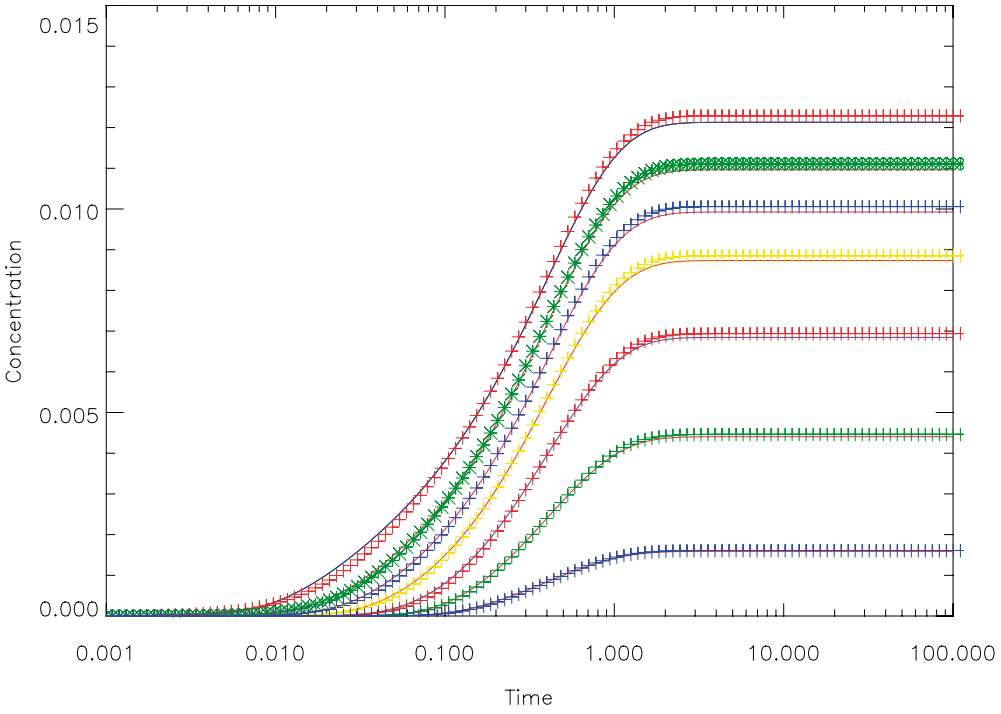

Figure 3-19. *This figure illustrates diffusion into a larger cylinder, with unit hole radius and relative cylinder dimension of 312.5/32. Agreement is again good.*

3.3 Additional analytic solutions

Recently, Neretnieks and his co-workers have published a number of papers that consider the problem of determining simple expressions for the groundwater flow rate, Q, and equivalent groundwater flow rate, Q_{eq}, for a fracture that intersects a canister located in fractured rock. This work is described in the following subsections.

3.3.1 Analytic solutions for a parallel plate fracture

This work has been reported by Liu and Neretnieks in /Liu and Neretnieks 2003/. The objective of this work was to obtain analytical solutions for Q and Q_{eq} for a parallel plate fracture that intersects a canister at the centre of the fracture. Note that the solutions are valid for any fracture orientation relative to the canister. The analytical solution for Q is:

$$Q = W b_c u_f f_u f_c \tag{40}$$

where

$$u_f = \frac{\rho g b_c^2}{12 \mu_w} \frac{\Delta h}{L} \tag{41}$$

and

$$f_u = \frac{1}{1 + \beta f_g} \tag{42}$$

and

$$f_c = 1 - \beta f_g \tag{43}$$

and

$$f_g = \frac{r_h}{r_s} \sqrt{\frac{w}{l}} \tag{44}$$

and

$$r_h = \frac{P_i}{2\pi} \tag{45}$$

and

$$r_s = \sqrt{\frac{S_i}{\pi}} \tag{46}$$

The nomenclature in these equations is as follows:

b aperture, m

b_c aperture of the parallel plate fracture, m

c_0 source concentration, mol m^{-3}

D diffusion coefficient, m^2 s^{-1}

l length of the inclusion in the direction parallel to fluid flow, m

L length of the fracture plane in the direction parallel to fluid flow, m

P_i perimeter of the inclusion, m

r radius of the canister, m

S_i area of the inclusion, m^2

w width of the inclusion in the direction normal to fluid flow, m

W width of the fracture plane in the direction normal to fluid flow, m

β ratio of the area of the inclusion to the area of the fracture plane

μ_w dynamic viscosity, Pa s

Using the same nomenclature, the equivalent flow rate, Q_{eq}, is given by

$$Q_{\text{eq}} = 8Db_c\sqrt{\frac{Pe}{\pi}} \tag{47}$$

where

$$Pe = \frac{u_f r_s}{D} f_u f_s \tag{48}$$

and

$$f_s = \frac{l+w}{2\sqrt{lw}} \tag{49}$$

and all other quantities are as defined above.

Liu and Neretnieks verified Equations (40) to (49) by undertaking a number of numerical studies of parallel plate fractures intersecting a canister, with a variety of fracture orientations relative to the axis of the canister. The results of the comparisons are shown in Figures 3-20 to 3-21.

Liu and Neretnieks have shown further that for flow parallel to the axis of the canister, the equivalent flow rate would be a factor 1.44 higher than the case for flow normal to the axis of the canister. On this basis, they argue that uncertainty in the direction and orientation of flow in fractures intersecting canisters should not play a key role in a safety case based on the KBS-3 concept.

Consideration should perhaps be given to the use of (47) and its supporting equations in future versions of COMP23. At the present time, use is made of Equation (25). It would then be of interest to compare the results, maybe in the form of additional test cases, that arise from these two approaches.

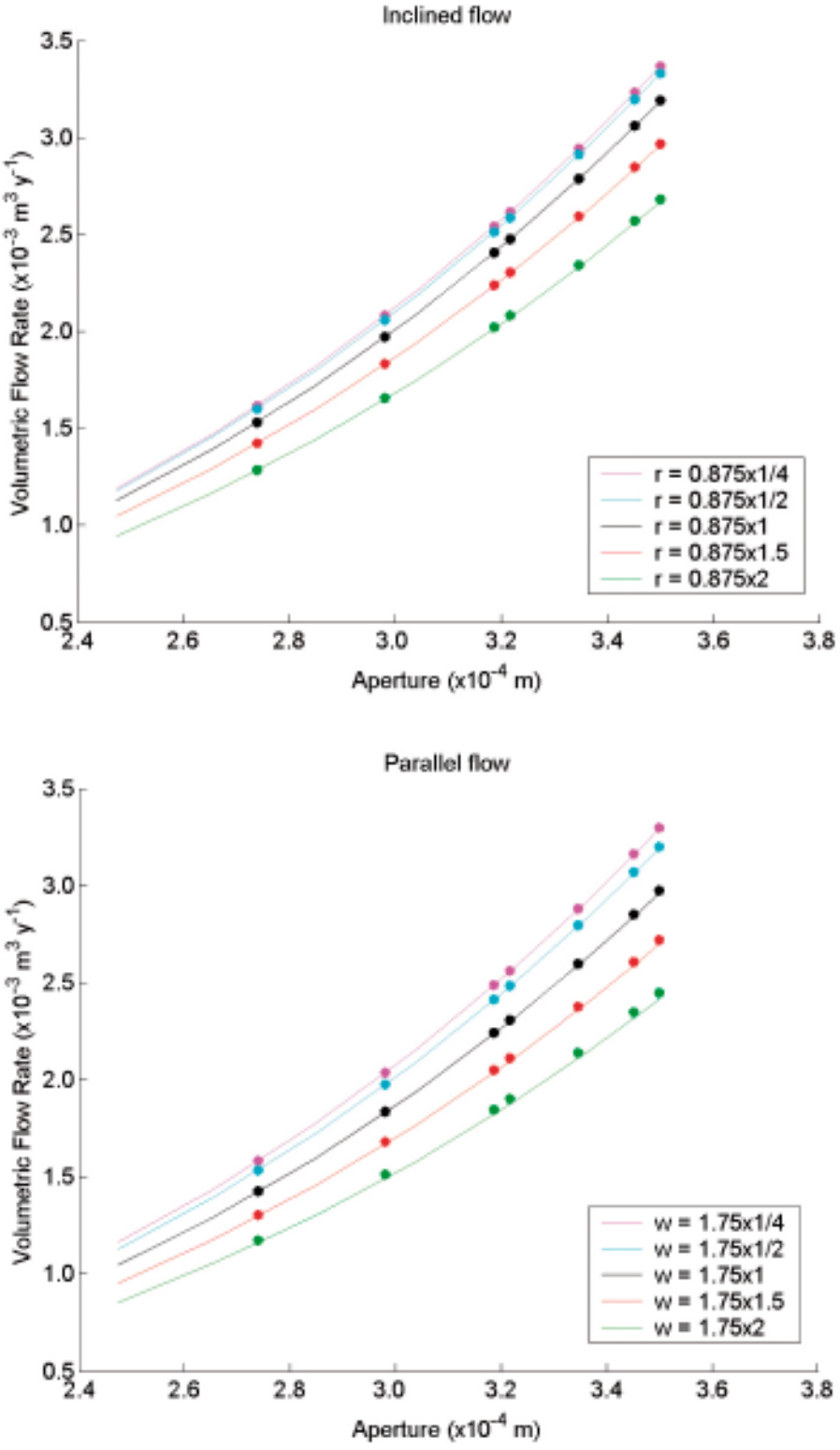

Figure 3-20. *The groundwater flow rate Q is plotted as a function of fracture aperture for inclined flow and parallel flow, for various canister parameter values. The numerical solution is represented by dots, and the analytical solutions by the continuous lines. It can be seen that the agreement is very close between numerical and analytical solutions.*

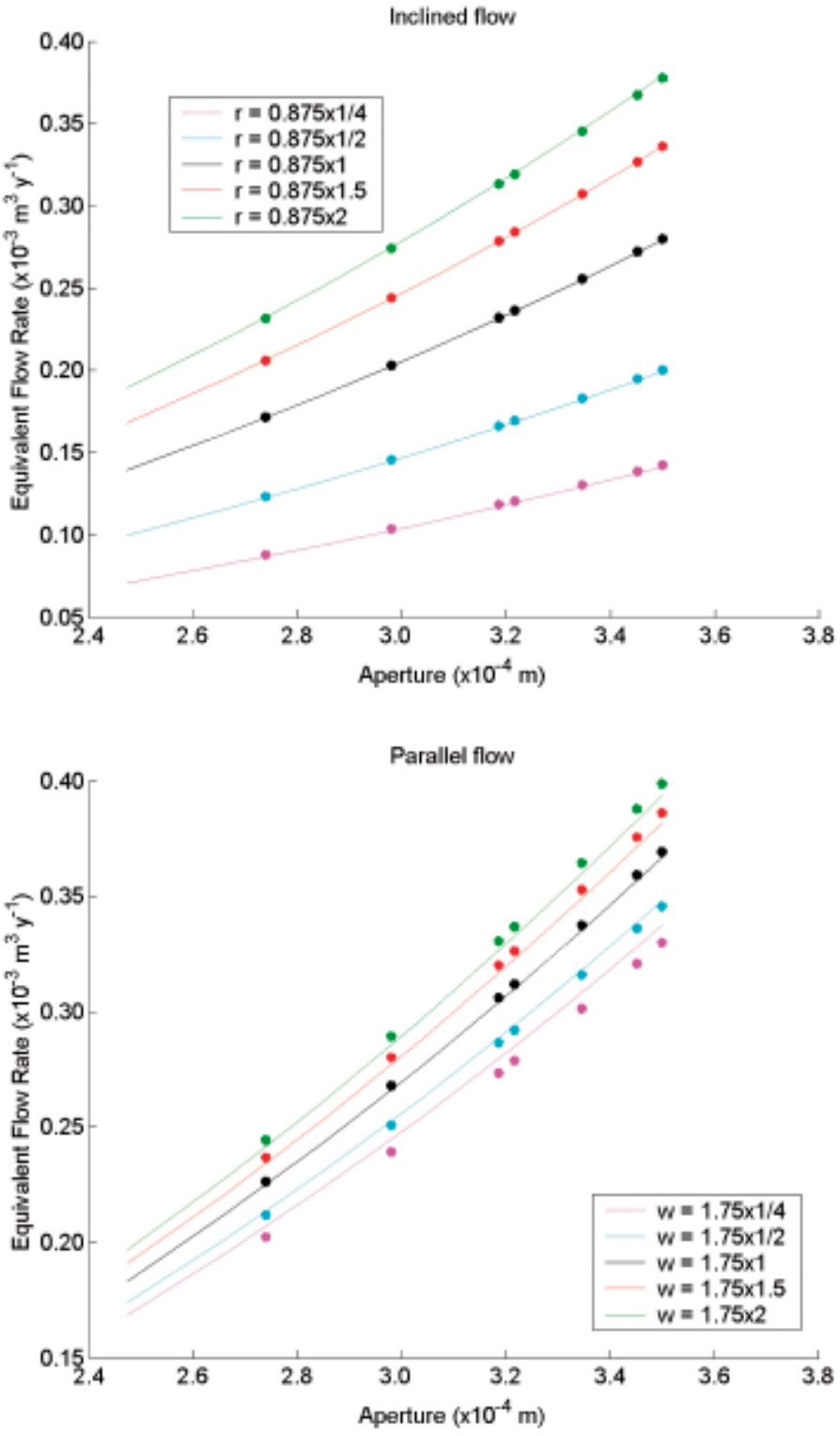

Figure 3-21. *The equivalent groundwater flow rate Q_{eq} is plotted as a function of fracture aperture for inclined flow and parallel flow, for various canister parameter values. The numerical solution is represented by dots, and the analytical solutions by the continuous lines. It can be seen that the agreement is very close between numerical and analytical solutions.*

3.3.2 Variable fracture apertures

Liu and Neretnieks extended the work of the previous section to consider a fracture intersecting a canister for which the fracture has spatially variable apertures. This work is reported in references /Liu and Neretnieks 2005ab/. In these works they considered two types of fracture: Gaussian fractures, in which the aperture distribution varies spatially according to a Gaussian autocovariance function, and fractal fractures, in which the spatial variation is specified by a power law power spectrum. In both cases, the distribution of apertures was described by log-normal probability density functions. An example of a fractal fracture realisation is shown in Figure 3-22.

Liu and Neretnieks generated a number of fracture realisations on the basis of the assumed aperture distributions, and computed the groundwater flow rates and equivalent flow rates for each realisation. Analysis of the results revealed a number of important conclusions:

1. For Gaussian fractures, the various fracture realisations led to distributions of volumetric and equivalent flow rate that are close to Normal distributions.
2. It was found that for any cases of flow through a single fracture of the Gaussian type, the hydraulic aperture determines the mean of the distribution of the volumetric flow rates, while the mechanical aperture determines the mean of the distribution of the equivalent flow rates. Thus, the parallel plate model /Liu and Neretnieks 2003/ may be used to predict the average properties of fluid flow and solute transport through natural fractures of the Gaussian type.

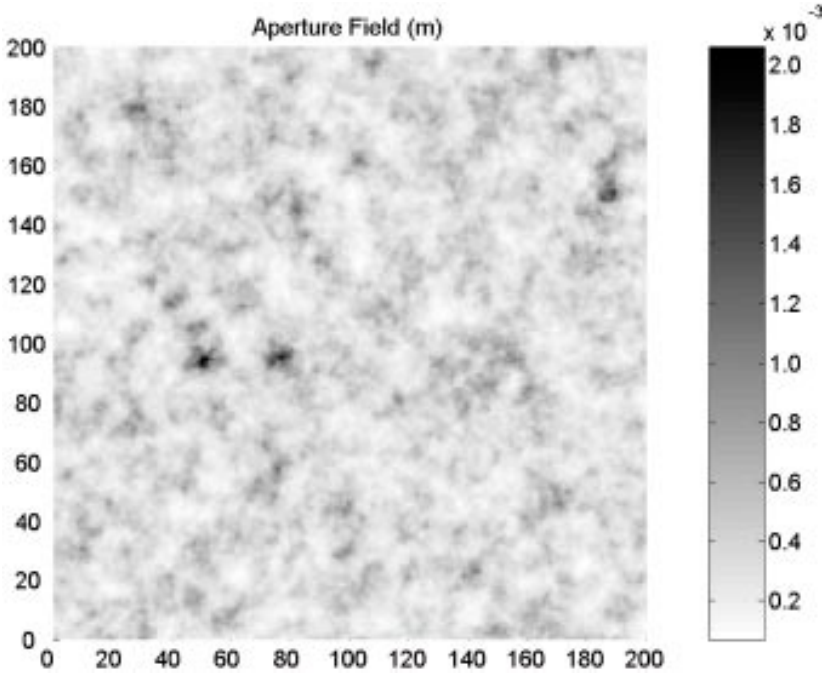

Figure 3-22. *Example of a fractal fracture realisation.*

3. The probability density function for the normalised volumetric flow rate for Gaussian fractures may be written in the form:

$$p\left(\frac{Q}{Q_{0,b=\mu}}\right) = N\left\{\left[1+\left(\frac{\sigma}{\mu}\right)^2\right]^{-3/2}, \quad C_v \frac{\sigma}{\mu}\frac{l}{L}\right\}$$

where l is a correlation length, L is the length of the fracture, μ is the mean of the fracture aperture distribution, σ is the standard deviation, and N represents a normal distribution. The first term in parentheses represents the mean of the Normal distribution, and the second term represents the standard deviation. C_v is a constant of proportionality that takes a value between 1.0 and 1.5.

4. A similar expression applies for fractal fractures, except that l is replaced by a "crossover dimension" and the value of C_v varies between 0.6 and 0.9.

5. The probability density function for the normalised equivalent flow rate for Gaussian fractures may be written in the form:

$$p\left(\frac{Q_{eq}}{Q_{eq,0,b=\mu}}\right) = N\left[1, \; C_{eq} \frac{\sigma}{\mu}\frac{l}{L}\right]$$

where the nomenclature is as above, except that the ratio of C_{eq} to C_v lies between 2 and 4.

6. A similar expression applies for fractal fractures, except that l is replaced by a "crossover dimension" and the ratio of C_{eq} to C_v lies between 2 and 4.

In conclusion, Liu and Neretnieks found that the distributions of the normalized volumetric and equivalent flow rates are both close to Normal, for both Gaussian and fractal fractures. This makes it possible to devise simple formulae to quantify the hydraulic behavior of natural fractures without making detailed calculations for every fracture intersecting a deposition hole or a tunnel.

4 Methods of solution

To represent the barrier system through which the species are transported, COMP23 makes use of the integrated finite-difference method /Narasimhan and Witherspoon 1976/ and of the concept of "compartments". The barrier system is discretized into compartments. Average properties over these compartments are associated with nodes within the compartment. From the theoretical point, of view the compartments may have any shape, but consist of only one material. The material balance over a compartment is given by:

$$\frac{\partial a_i^n}{\partial t} = \sum_j g_{i,j} c_j^n - \lambda_n a_i^n + \lambda_{n,n-1} a_i^{n-1} \tag{50}$$

where a_i^n is the amount of nuclide n in compartment i, c_i^n is the concentration of nuclide n in the pore water in compartment i, λ_n and $\lambda_{n,n-1}$ are parent and daughter decay constants, and $g_{i,j}$ is the transport coefficient linking compartments i and j. The concentration, c_i^n, where $\mathrm{n} \in \mathrm{S_E}$ (i.e. nuclide n is an isotope of element E), is related to a_i^n by

$$c_i^n = \begin{cases} \dfrac{a_i^n}{V_i K_{E,i}} & \text{if } a_{E,i}^T \le V_i K_{E,i} c_E^S \\ \dfrac{c_E^S a_i^n}{a_{E,i}^T} & \text{if } a_{E,i}^T > V_i K_{E,i} c_E^S \end{cases} \tag{51}$$

where $K_{E,i}$ is the distribution coefficient for element E in compartment i, V_i is the volume of compartment i, $a_{E,i}^T$ is the total amount of element E in compartment i and c_E^S is the solubility limit for the solubility group, S_E, of element E. $K_{E,i}$ is given by

$$K_{E,i} = \varphi_{E,i} + (1 - \varphi_{E,i}) k_{E,i}^d \rho_i \tag{52}$$

where $\varphi_{E,i}$ is the porosity for element E in compartment i, $\tilde{n}_i$ is the density of the solid material in compartment i and $k_{E,i}^d$ is the sorption coefficient for element E in compartment i. $a_{E,i}^T$ is given by

$$a_{E,i}^T = \sum_{m \in S_U} a_i^m . \tag{53}$$

The diffusional contribution to $g_{i,j}$ is expressed in terms of diffusional resistances. Each compartment makes a contribution to this resistance. The diffusional resistance from compartment i to compartment j is $R_{i,j}$ where

$$R_{i,j} = \frac{R_i}{2} + \frac{R_j}{2}, \tag{54}$$

and R_i and R_j depend on the direction of transport and the nuclide (through the diffusion coefficient). R_i takes the form

$$R_i = \frac{l_w}{A_w D_{e,i}^n} \tag{55}$$

where l_w is the length of the compartment in the transport direction (w can be either x, y or z), A_w is the cross-sectional area of the compartment normal to the direction of transport and $D_{e,i}^n$ is the effective diffusion coefficient for nuclide n in compartment i. Additional resistances can be added to model special situations, such as transport from a small compartment into a large one (see the following sections).

The diffusional contribution to $g_{i,j}$ may now be written in terms of $R_{i,j}$ as

$$g_{i,j} = \begin{cases} \dfrac{1}{R_{i,j}} & \text{if } i \neq j \\ -\displaystyle\sum_{j \neq i} g_{i,j} & \text{if } i = j \end{cases} . \tag{56}$$

The elements required to define the compartmentalization are the geometry of the system, dimensions of the system and the type of material. The compartments are defined by their volume, their diffusion length and cross-sectional area. Conceptually, the model uses a rather straightforward compartmentalization process. This coarse compartmentalization could yield poor or even meaningless numerical results. To avoid this, analytical or semi-analytical solutions are introduced in the model in zones where a finite-difference scheme would require a fine discretization to obtain an accurate result. Some of the approaches used by the model to describe the solute transport in these sensitive zones are shown below.

5 Verification and building confidence

In order to build confidence that COMP23 is providing credible results for radionuclide migration and transport problems in the near field, a series of test cases have been undertaken and the results documented. A summary of the test cases is set out in the Table 5-1.

The tests can be seen to cover three types of test:

1. Code comparisons. A particular feature of COMP23 is checked by comparing the results from COMP23 with a separate code that is designed to undertake the same computations.
2. Plausibility checks. A particular feature of COMP23 is checked by examining the results and ensuring that they are physically plausible and in line with what would be expected.
3. Analytic solution. The output from COMP23 is checked against the results of a known analytic solution that describes the system being modelled.

In carrying out these tests, no serious discrepancies were found. Some artefacts of using a compartmental approach to model a "continuous" system were seen in some of the tests, but these are not considered to be serious issues.

Table 5-1.

Test case	Objective of the test case	Method of testing
1	Solubility limited source term	Code comparison
2	Solubility limited source term, increased number of compartments	
3	Congruent dissolution from source	Code comparison
4	Transport into a flowing feature	Code comparison
5	Transport through a small hole in canister wall	Code comparison
6	Transport through a large hole in canister wall	Code comparison
7	Transport through a canister hole with increasing size (ramp)	Code comparison
8	Transport through a canister hole with increasing size (step)	Plausibility check
9	One-dimensional diffusion in a medium bounded by two parallel planes (comparison with analytical solution)	Analytic Solution
10	Calculation case from SR 97, Aberg pessimistic canister related parameters	Plausibility check
11	Calculation case from SR 97, Aberg special case with immediate fuel dissolution, IRF=1	Plausibility check
12	Output in Bq instead of mol	Plausibility check
13	FUELSURFACE dissolution model	Plausibility check
14	Dissolution due to alpha radiolysis – decay model	Plausibility check
15	Dissolution due to alpha radiolysis – explicit model	Plausibility check
16	Shared solubility	Plausibility check
17	Probabilistic calculation	Plausibility check
18	Calculation case from SR 97, Aberg pessimistic canister related parameters, shared solubility	Plausibility check
19	Consistency check when multiple FARF31 modules are used	Plausibility check
20	Time-dependent variations to sorption coefficient	Analytic Solution
21	Time-dependent variations to porosity	Analytic Solution
22	Time-dependent variations to diffusion coefficient	Analytic Solution
23	Time-dependent variations to solubility limits	Code comparison
24	Material-dependent solubility limits	Code comparison

6 Documentation and administration

6.1 Documentation

COMP23 has been documented in three reports that provide information on the conceptual basis of the model, instructions on how to use the model, and test cases developed to build confidence in the model /Romero et al. 1995, Cliffe and Kelly 2004, Lindgren et al. 2006/. These reports are:

1. Fast Multiple-Path Model to calculate Radionuclide Release from the Near Field of a Repository, published in Radioactive waste management, 1995.
2. COMP23 version 1.2.1 User's Manual, updated in August 2004.
3. COMP23 Test Batch, updated in July 2005.

The first of these reports provides the technical basis for COMP23. The user manual describes how to use the COMP23 programme and how to set up the input data files. The test batch documents sets out in detail the descriptions and results of the test cases described in Chapter 4.

6.2 Quality control

The development of COMP23 is undertaken using the Unix Source Code Control System (SCCS). Under the SCCS system, it is possible to keep track of every modification, and to return to an earlier version of the code if necessary. SCCS is structured so that the developer always works with a copy of the latest version of a particular piece of code. Any new developments can then be checked by running any available test cases. If the revised code passes the test cases, then the main source code can be updated within SCCS and the modification id recorded.

6.3 Development using test cases

As described in Chapter 4, a number of test cases have been set up to build confidence that COMP23 is functioning as intended. The tests cover simplified cases that can be compared with analytic solutions, as well as more complex cases that can be checked against the output of other independent computer codes.

An important objective of the test batch is to provide results to be run after a code modification and hence verify that the new version is giving the expected results. After a code modification is made, the test batch should be executed to check that the results are the same as prior to the modification of the code. By running the test batch, several different features of the code are tested.

7 References

Cliffe K A, Kelly M, 2004. COMP23 Version 1.2.1 User's Manual. SKB TR-04-64, Svensk Kärnbränslehantering AB.

Haworth A, Ilett D J, Thompson A M, Worth D J, 1996. Developments to the NUCTRAN Computer Program.

Haworth A, Thompson A M, Worth D J, 1997. Developments to the PROPER Version of NUCTRAN.

Lindgren M, Pettersson M, Cliffe A, Kelly M, 2006. COMP23 Test Batch, Kemakta Konsult. SKB R-06-112, Svensk Kärnbränslehantering AB.

Liu L, Neretnieks I, 2003. Fluid Flow and Solute Transport Through a Fracture Intersecting a Canister – Analytical Solutions for the Parallel Plate Model, Proc. Scientific Basis for Nuclear Waste Management XXVII, Kalmar, Sweden, June 15–19, 2003, p. 749, Materials Research Society.

Liu L, Neretnieks I, 2005a. Analysis of Fluid Flow and Solute Transport in a Fracture Intersecting a Canister with Variable Aperture Fractures and Arbitrary Intersection Angles, Nuclear Technology, Volume 150.

Liu L, Neretnieks I, 2005b. Analysis of Fluid Flow and Solute Transport through a Single Fracture with variable Apertures Intersecting a Canister: Comparison between Fractal and Gaussian Fractures, presented at the MRS 2005 Conference, Belgium.

Narasimhan T N, Witherspoon P A, 1976. An Integrated Finite Difference Method for Analyzing Fluid Flow in Porous Media, Water Resour. Res., 12, 57.

Neretnieks I, 1982. Leach Rate of High Level Waste and Spent Fuel-Limiting Rates as Determined by Backfill and Bedrock Conditions, Proc. Scientific Basis for Nuclear Waste Management V, Berlin, Germany, June 7–10. 1982, W.Lutze, Ed., p. 559.

Neretnieks I, 1986. Stationary Transport of Dissolved Species in the Backfill Surrounding a Waste Canister in Fissured Rock: Some Simple Analytical Solutions, Nucl. Technol., 72–194.

Romero L, Moreno L, Neretnieks I, 1995. Fast Multiple-Path Model to Calculate Radionuclide Release from the Near Field of a Repository, Nucl. Technol., 112, 89.

Serco Assurance. http://www.sercoassurance.com/entwife/main.html

Werme L, Sellin P, Forsyth R, 1990. Radiolytically Induced Oxidative Dissolution of Spent Nuclear Fuel. SKB TR-90-08, Svensk Kärnbränslehantering AB.